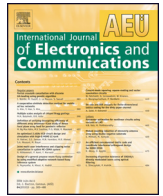




Contents lists available at ScienceDirect

International Journal of Electronics and
Communications (AEÜ)journal homepage: www.elsevier.com/locate/aeue

REGULAR PAPER

CMOS design of a low power and high precision four-quadrant analog multiplier

Naser Beyraghi*, Abdollah Khoei

Microelectronics Research Laboratory, Urmia University, Urmia 57159, Iran

ARTICLE INFO

Article history:

Received 29 May 2014

Accepted 18 October 2014

Keywords:

CMOS analog multiplier

Four quadrant

Squarer circuit

Current mode

ABSTRACT

In this paper, a novel current-mode Four-quadrant analog multiplier is proposed. The newly designed current squarer circuits and one current mirror which all operate in low supply voltage (2 V) are the basic building blocks in realization of the mathematical equations. The multiplier circuit is designed by using 0.35 μm standard CMOS technology and to validate the circuit performance, the proposed multiplier has been simulated in HSPICE simulator. The simulation results demonstrate a linearity error of 0.17%, a THD of 0.16% in 1 MHz, a -3 dB bandwidth of 485 MHz and a maximum power consumption of 0.232 mW while the static power consumption is 0.111 mW.

© 2014 Published by Elsevier GmbH.

1. Introduction

Analog multiplier is an important building block for many applications such as adaptive filters, frequency doublers, modulators, neural networks, fuzzy logic controllers, etc. Due to the popularity of CMOS technology, MOS transistors are the first choice for the device fabrication. Therefore, many CMOS analog multipliers which exploit MOS transistors have been presented in the literature. Among the various available methods for implementing a continuous time current-mode analog multiplier, those who utilize transistors operating in saturation or linear [1–6] regions are more prevalent than those who are in sub-threshold [7–10] region. Although in the former method power consumption is higher, the other features like dynamic range of input and output currents, operating frequency and linearity are much better in comparison to the later method. Moreover, class AB current-mode cells are used as the other approach of the multiplier implementation [11,12] where the transconductance parameter of the PMOS and the NMOS transistors should be identical. Otherwise, the output current will not be multiplied correctly and consequently the total harmonic distortion can be a considerable shortcoming. On the other hand, having identical transconductance parameter is very difficult, because its value is strongly depended on the fabrication process and varies lot by lot [3]. By using saturated transistors, we can use the inherent square-law characteristic of MOS transistors in saturation region,

which are utilized for construction of current-mode squarer and square root circuits. Thus, multipliers can take the advantage of either square root circuits [5,6,13–15] or squarer circuits [4,16–18] in their structures.

In this paper, squarer circuits have been used. Since the current squarer circuit is the core cell of the multiplier circuit, it is considered as the main element in determining of the multiplier functionality level. Hence, we present a low power, high speed and high precision four-quadrant current-mode analog multiplier circuit based on a newly designed current squarer circuit. The circuit works under supply voltage of $V_{DD} = 2$ V. The squarer circuit has been designed based on the square-law characteristic of an MOS transistor operated in the saturation region. Proposed multiplier is composed of four squarer cells and a current mirror so that it has a symmetrical structure and results a low harmonic distortion. Simulations are performed by HSPICE simulator and results imply that high linearity, high speed, wide bandwidth and low power dissipation are the main advantages of proposed multiplier.

2. Circuit description

2.1. Current-mode squarer circuit

Squarer circuits are widely used in communication systems and measurements such as frequency doublers, peak amplitude detector and analog multipliers. Square circuits can be categorized into three groups proportional to the type of their input signals: voltage-mode [19,20], current-mode [3,4,16,21–23] and mixed signals [24]. One of the most effective methods in decreasing power dissipation is lowering supply voltage level, but designing in this situation is

* Corresponding author. Tel.: +98 9141450495.

E-mail addresses: n.beyraghi@gmail.com (N. Beyraghi), a.khoei@mail.urmia.ac.ir (A. Khoei).

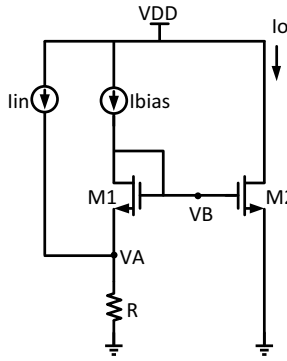


Fig. 1. Proposed current squarer circuit.

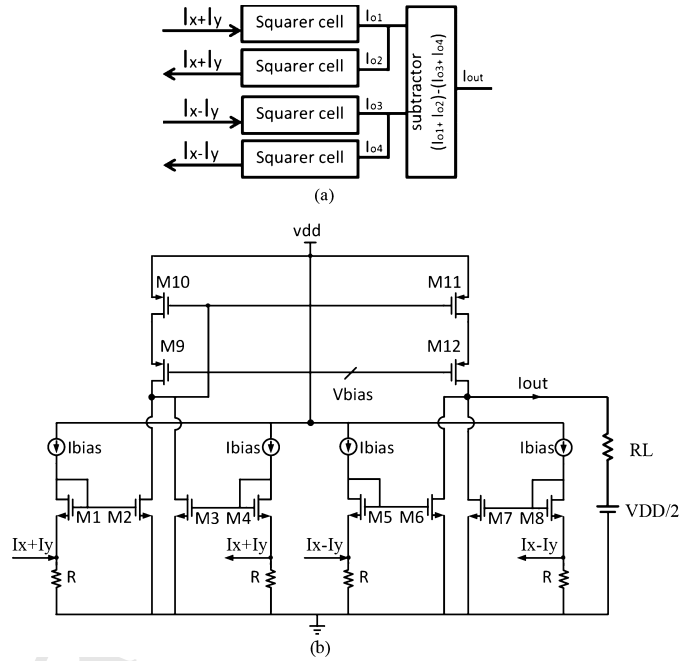


Fig. 2. Proposed multiplier structure (a) block diagram and (b) circuit level.

I_{in} is the current input signal and I_{bias} is a suitable constant current which sets the initial voltage of node (B) (i.e. V_0 when $I_{in} = 0$). Voltage of node (B) is

$$V_B = R(I_{in} + I_{bias}) + V_{t1} + \sqrt{\frac{2I_{bias}}{K1}} \quad (3)$$

$$V_0 = RI_{bias} + V_{t1} + \sqrt{\frac{2I_{bias}}{K1}} \quad (4)$$

$$V_E = V_0 - V_{t2} \quad (5)$$

According to above equations, Eq. (1) will be changed into Eq. (6).

$$I_o = k(RI_{in} + V_0 - V_{t2})^2 = k(RI_{in} + V_E)^2 \quad (6)$$

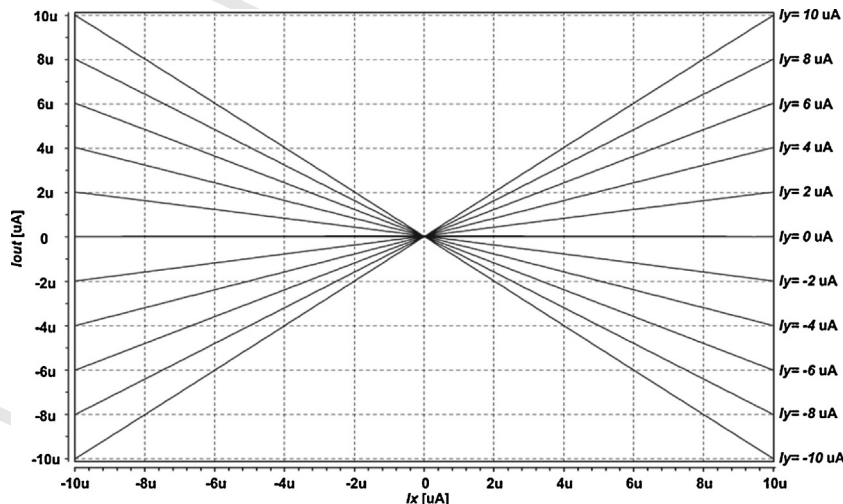


Fig. 3. DC transfer characteristic of proposed four-quadrant multiplier.

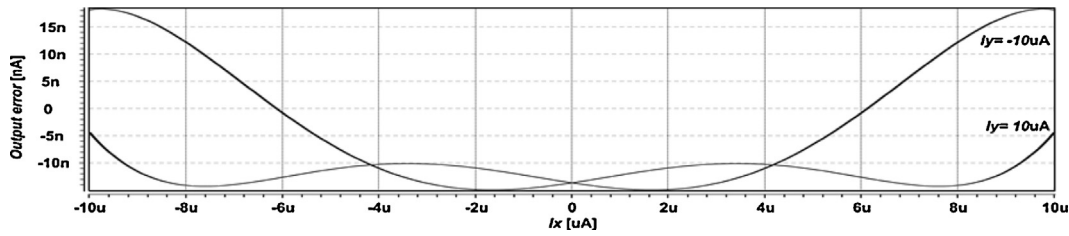


Fig. 4. Linearity error when $I_Y = \pm 10 \mu\text{A}$.

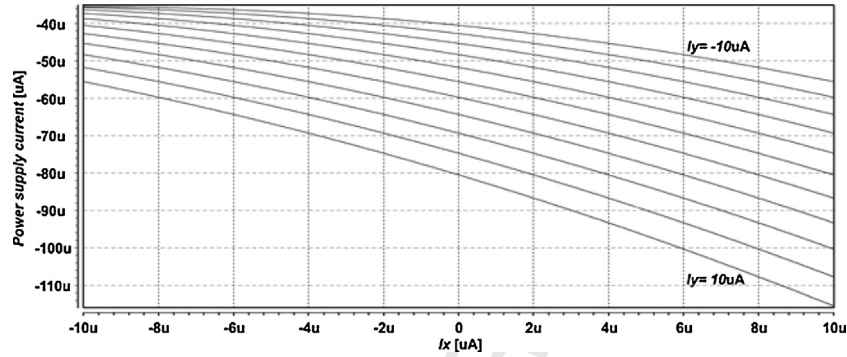


Fig. 5. Drained currents from power supply (VDD).

2.2. Multiplier circuit

To implement the proposed multiplier, four numbers of squarer cells are required in its structure. According to Eq. (6), if $I_X + I_Y$, $-(I_X + I_Y)$, $I_X - I_Y$ and $-(I_X - I_Y)$ are applied as their input currents, the output currents of these circuits will be

$$I_{o1} = k(R(I_X + I_Y) + V_E)^2 \quad (7)$$

$$I_{o2} = k(-R(I_X + I_Y) + V_E)^2 \quad (8)$$

$$I_{o3} = k(R(I_X - I_Y) + V_E)^2 \quad (9)$$

$$I_{o4} = k(-R(I_X - I_Y) + V_E)^2 \quad (10)$$

The output current of multiplier is given by subtracting the summation of I_{o1} and I_{o2} from summation of I_{o3} and I_{o4} as follows:

$$I_{out} = (I_{o1} + I_{o2}) - (I_{o3} + I_{o4}) = 8kR^2 I_X I_Y \quad (11)$$

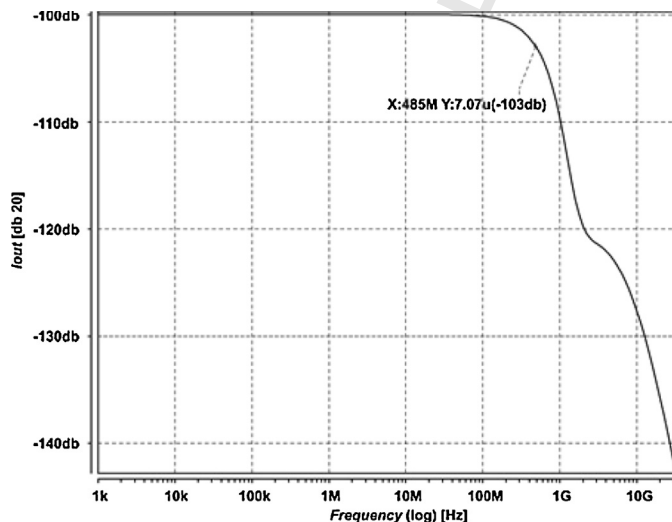


Fig. 6. AC characteristic of proposed multiplier.

This idea is shown schematically in the form of block diagram and transistor level structure in Fig. 2.

2.3. Analysis of the performance of multiplier

In this section, the effects of various mismatches which can be caused by process variations have been surveyed on the performance of proposed multiplier.

2.3.1. Input current mismatch

Assume that both of the input currents (I_X and I_Y) are different from the ideal desired value and are defined as follows:

$$I_X = I_{xideal} + \Delta I_{xideal} \quad (12)$$

$$I_Y = I_{yideal} + \Delta I_{yideal} \quad (13)$$

$$\Delta = \frac{n}{100} \quad (14)$$

Substituting Eqs. (12) and (13) into Eq. (11) results in

$$\begin{aligned} I_{out} &= 8kR^2(I_{xideal} + \Delta I_{xideal})(I_{yideal} + \Delta I_{yideal}) = 8kR^2 I_{xideal} I_{yideal} \\ &\quad + 8kR^2(I_{xideal} \Delta I_{yideal} + I_{yideal} \Delta I_{xideal} + \Delta I_{xideal} \Delta I_{yideal}) \\ &= 8kR^2(I_{xideal} I_{yideal} + I_{Error}) \end{aligned} \quad (15)$$

Whenever input signals are $I_{xideal} = I_{yideal} = A$, I_{Error} , will be

$$I_{Error} = \frac{2nA^2}{100} + \left(\frac{nA}{100}\right)^2 \quad (16)$$

In this equation the second term is much smaller than the first term and can be ignored, so for 1% mismatch ($n=1$) the percentage of output error is

$$Error = \frac{I_{Error}}{I_{out}} \times 100 = 2n\% = 2\% \quad (17)$$

Note that obtained error is for the worst case when the mismatch of I_X and I_Y both are in a similar direction.

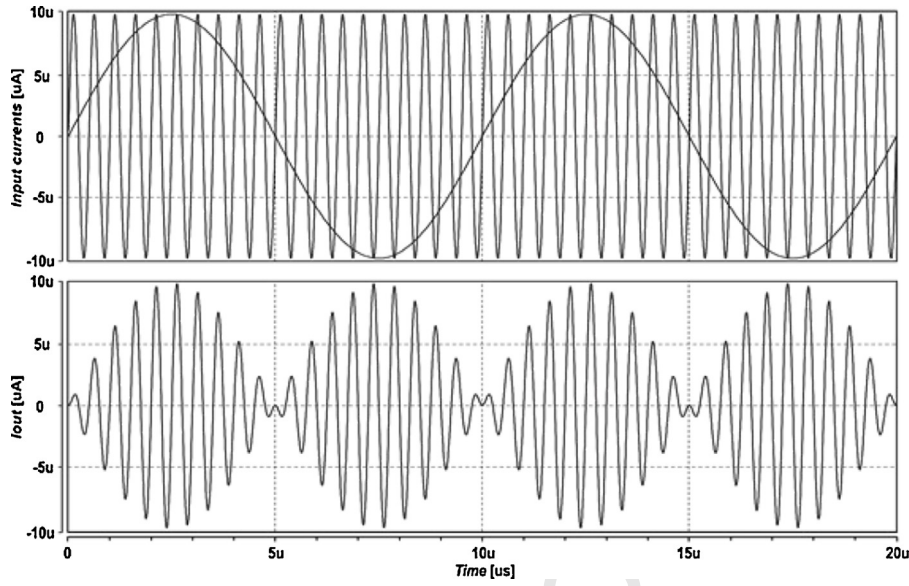


Fig. 7. Multiplier as a modulator.

2.3.2. Threshold voltage mismatch

According to Eq. (5), V_E is a function of V_{th} . Thus, the variation of threshold voltage will change the value of V_E . V_E is a common parameter for the squarer cells which are used in multiplier circuit. Consequently, by symmetrical structure of proposed multiplier V_E is eliminated in Eq. (11) and will not appear in the output current. In addition, the threshold voltage variation changes the initial value of node (B) (i.e. V_0) as shown in Eq. (4). Therefore, to preserve the accuracy of output current in an acceptable level, the value of V_0 must be fixed in its initial value by adjusting the bias current value (I_{bias}) so that by increasing the threshold voltage, the bias current should be decreased and vice versa.

2.3.3. Transconductance parameter mismatch

In the ideal case, M_2 , M_3 , M_6 and M_7 have identical dimensions and are match. But now, assume that the transconductance for M_2 and M_7 is K_2 and for M_3 and M_6 is K_1 where

$$k_2 = k_1 + \Delta k_1 \quad (18)$$

In this condition, the output current is obtained by Eq. (19).

$$\begin{aligned} I_{out_{real}} &= 4(k_1 + k_2)R^2 I_X I_Y = 4(2k_1 + \Delta k_1)R^2 I_X I_Y = 8k_1 R^2 I_X I_Y \\ &\quad + 4\Delta k_1 R^2 I_X I_Y = 8k_1 R^2 I_X I_Y + \frac{4nK_1}{100} R^2 I_X I_Y \\ &= I_{out_{ideal}} + I_{Error} \end{aligned} \quad (19)$$

According to Eq. (19), the percentage of output current error caused by transconductance mismatch can be calculated as follows:

$$Error = \frac{I_{Error}}{I_{out}} \times 100 = \frac{nI_X I_Y}{200I_X I_Y} = \frac{n}{200} \% \quad (20)$$

For 1% mismatch ($n = 1$) the percentage of output error is 0.5%.

The low input and high output impedances cause good impedance conformity for current-mode circuits. The input and output impedances of proposed multiplier are

$$R_{in} = (R||\infty) = R \quad (21)$$

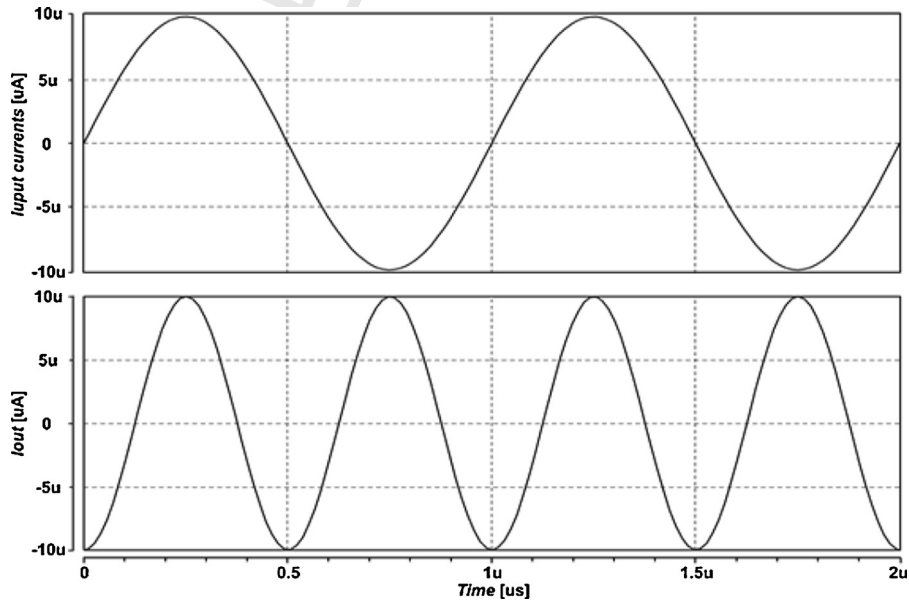


Fig. 8. Multiplier as a frequency doubler.

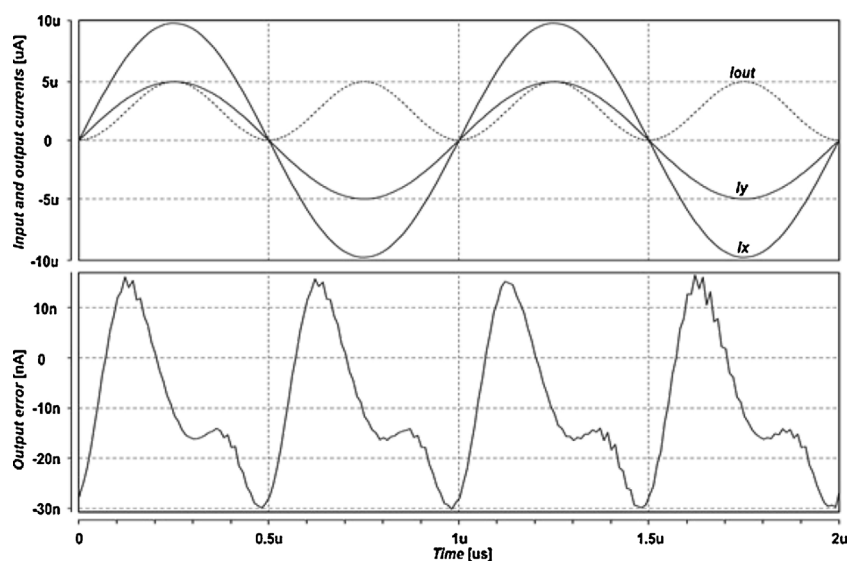


Fig. 9. Simulation of multiplier for transient error measurement.

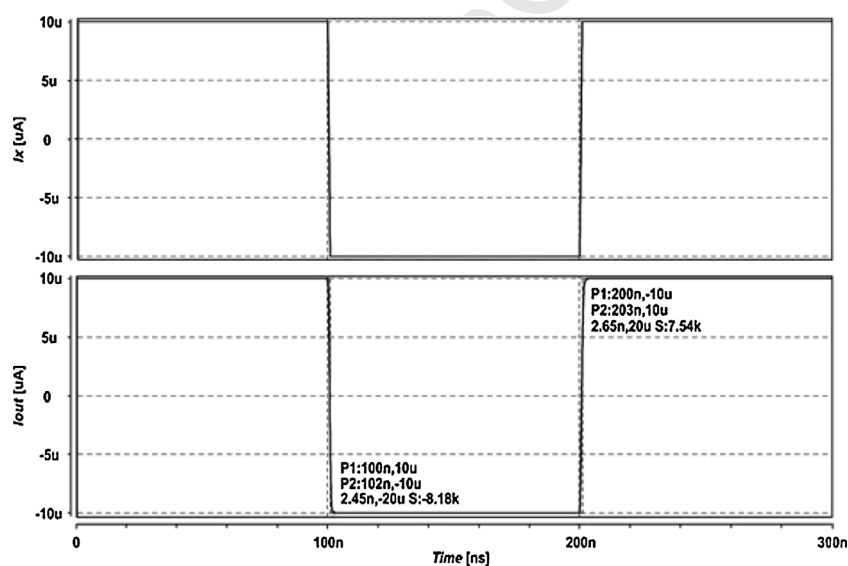


Fig. 10. Pulse response of multiplier.

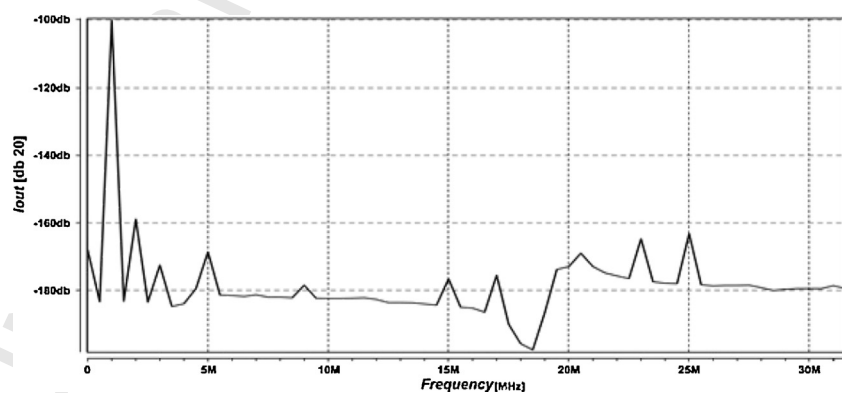


Fig. 11. Output spectrum of multiplier.

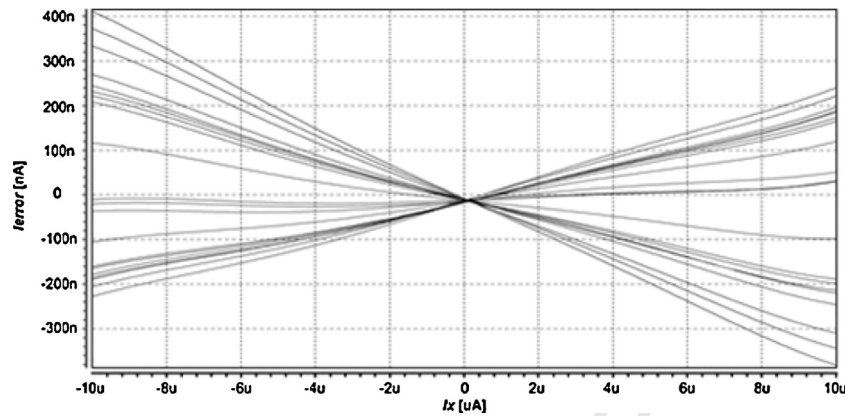


Fig. 12. Output error due to Monte Carlo analysis for transconductance parameter variations.

Table 1
Sizes of the transistors used in the proposed current-mode multiplier.

Transistors	Aspect ratio W/L ($\mu\text{m}/\mu\text{m}$)
M2, M3, M6, M7	1.4/1
M1, M4, M5, M8	1/1
M9, M10, M11, M12	6/0.5

Table 2
The total harmonic distortion (THD) versus input signal (I_X) peak to peak amplitude at different frequencies.

Amplitude	10 kHz	100 kHz	1 MHz	10 MHz
$\pm 5 \mu\text{A}$	−61.5 db	−59.2 db	−56.8 db	−44.8 db
$\pm 10 \mu\text{A}$	−58.9 db	−56.9 db	−55.8 db	−43.7 db
$\pm 15 \mu\text{A}$	−46.8 db	−46.7 db	−46.5 db	−41.2 db

To study the power efficiency of proposed circuit, drained currents from VDD are shown in Fig. 5. According to Fig. 5, the maximum power dissipation is 232 μW when I_X and I_Y are 10 μA (drained current = 116 μA). However, the quiescent power consumption is 111 μW when I_X and I_Y are zero (drained current = 55.5 μA). The frequency characteristic of the multiplier where I_Y is set to 10 μA DC and I_X is the AC-varying signal with 10 μA magnitude, is shown in Fig. 6 and exhibits a −3 dB bandwidth of 485 MHz. Fig. 7 demonstrates the use of the multiplier as an analog amplitude modulator where I_X is the sinusoidal modulating signal with magnitude equal to $\pm 10 \mu\text{A}$ and frequency ($F_x = 100 \text{ kHz}$) while I_Y is the sinusoidal carrier with amplitude equal to $\pm 10 \mu\text{A}$ and frequency ($F_y = 2 \text{ MHz}$). Fig. 8 shows the use of the multiplier as a frequency doubler where both I_X and I_Y are sinusoidal signals with magnitude equal to $\pm 10 \mu\text{A}$ and frequency ($F = 1 \text{ MHz}$).

In order to study the linearity error in a transient condition and to do an equitably comparison with [4,17], another simulation in which the input current are similar to the currents used in [4,17], was performed. The simulation result is displayed in Fig. 9 revealing a linearity error of 0.24% which is smaller than referred works. Fig. 10 shows the pulse response of multiplier where I_Y is set to 10 μA and I_X is a pulse with amplitude equal to $\pm 10 \mu\text{A}$ and frequency ($F_x = 5 \text{ MHz}$). Proportional to the variation of I_X , the settling times are 2.65 ns and 2.45 ns for raising and falling edges, respectively. Fig. 11 shows the spectrum of the output current when I_Y is fixed at 10 μA and I_X is a 1 MHz sinusoidal with peak to peak amplitude of $\pm 10 \mu\text{A}$ and indicates that the other harmonic components are about 60 dB below the fundamental component. Monte Carlo analysis is usually utilized to model random mismatches between different components due to process variation. Figs. 12 and 13

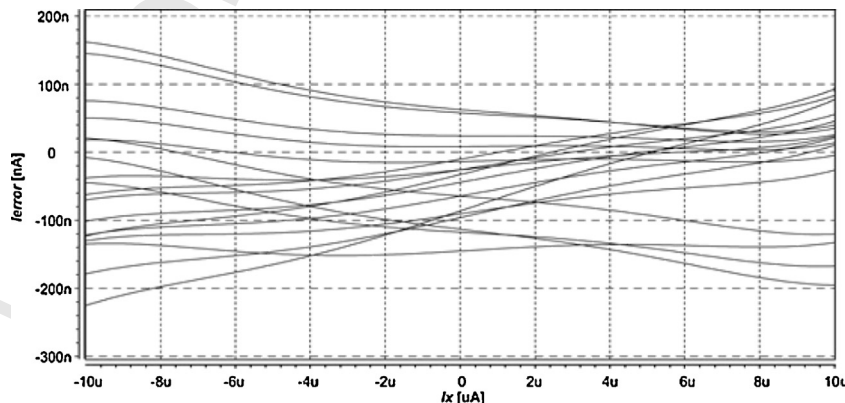


Fig. 13. Output error due to Monte Carlo analysis for threshold voltage variations.

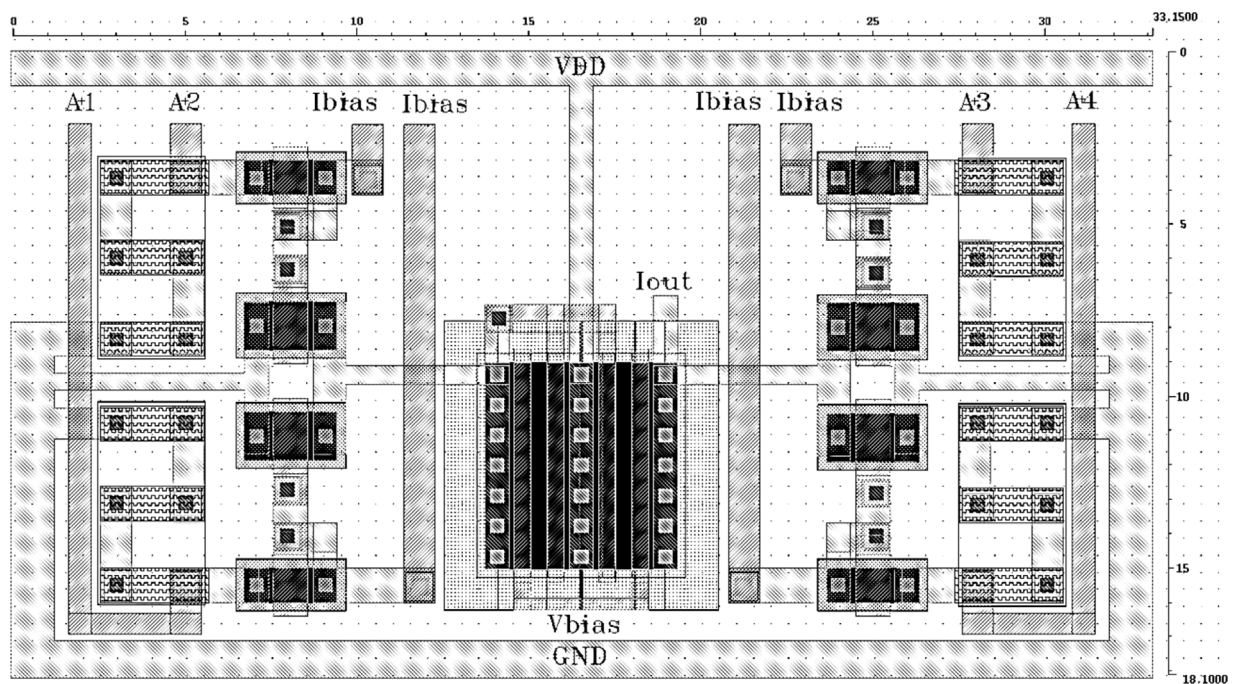


Fig. 14. Layout of proposed multiplier.

Table 3
Comparison between this work and previous works.

Reference	Technology (μm)	Supply voltage (V)	Input range (μA)	Output range (μA)	Linearity error (%)	THD, 1 MHz 20 μA (%)	Power consumption (μW)	Chip area (μm^2)	–3 db bandwidth (MHz)
[3]	2	5	± 20	± 5	1.22	1.54	930	–	22.4
[4]	0.35	3.3	± 10	± 10	1.1	0.97	340	872	41.8
[5]	2.4	5	100	100	1.2	1 (10 kHz)	700	32×10^4	12.3
[14]	0.35	3	10	20	–	0.14	–	10^4	44
[16]	0.5	± 1.5	± 60	± 7	3.9	4.485	720	–	31
[17]	0.25	3.3	± 10	± 10	0.56	0.96	214.5	234.9	533
[25]	0.5	± 1.5	± 20	± 10	1.2	3.7	460	–	19
[26]	0.8	1.5	± 15	± 10	–	0.9	(1 kHz)	184	5.5
[27]	0.18	1.2	10	40	0.75	–	60	600	79.6
[28]	0.5	± 1.5	± 50	± 25	0.9	0.44 (20 kHz)	600 (static)	–	205
[29]	0.25	1.5	± 200	± 40	0.8	0.25	–	–	154
[30]	0.35	± 0.75	± 20	± 20	–	0.83 (10 MHz)	–	186×10^2	140
This work	0.35	2	± 10	± 10	0.17	0.16	232	594	485

clarify that the maximum linearity error is less than 4% and 2% when the Monte Carlo analysis is performed for transconductance parameter and V_{th} , respectively. The total harmonic distortion (THD) versus input signal (I_X) peak to peak amplitude at 10 kHz, 100 kHz, 1 MHz and 10 MHz is shown in Table 2 when I_Y is 10 μA . Table 2 makes it clear that the THD is much better in this work than the previous works. This THD improvement originates from the symmetrical structure of proposed multiplier.

A comprehensive comparison between the performance of multipliers reported in the previous works and proposed multiplier is presented in Table 3. Based on this comparison, especially with those works have been designed in a similar process (0.35 μm), features like small linearity error, low harmonic distortion, wide bandwidth, high speed and low power consumption can be cited as the advantage of proposed multiplier.

4. Conclusion

A current-mode four-quadrant multiplier based on a newly designed squarer circuit was proposed. The simulation results indicate that the symmetrical configuration of proposed circuit allows

us to achieve a high linearity. The other advantages of proposed circuit were verified by various simulation results. The layout of this circuit which is depicted in Fig. 14 has been drawn by Cadence Virtuoso software and illustrates that the occupied area is about 594 μm^2 .

References

- [1] Seng YK, Rofail SS. Design and analysis of a ± 1 V CMOS four-quadrant analogue multiplier. *IEEE Proc Circuits Dev Syst* 1998;145(3):148–54.
- [2] Suzuki T, Oura T, Yoneyama T, Asai H. A new CMOS 4Q-multiplier using linear and saturation regions complementally. In: *Proceedings of solid-state circuits conference, ESSCIRC*; 2002. p. 755–8.
- [3] Tanno K, Ishizuka O, Tang Z. Four-quadrant CMOS current-mode multiplier independent of device parameters. *IEEE Trans Circuit Syst II* 2000;47(5):473–7.
- [4] Naderi A, Khoei A, Hadidi K, Ghasemzadeh H. A new high speed and low power four-quadrant CMOS analog multiplier in current-mode. *AEU – Int J Electron Commun* 2009;63(9):769–75.
- [5] Lopez-Martin AJ, Carlosena A. Current-mode multiplier/divider circuits based on the MOS translinear principle. *Analog Integr Circuits Signal Process* 2001;28(3):265–78.
- [6] Lopez-Martin AJ, De La Cruz Bias CA, Ramirez-Angulo J, Carvajal RG. Compact low-voltage CMOS current-mode multiplier/divider. In: *Proceedings of IEEE international symposium on circuits and systems (ISCAS)*; 2010. p. 1583–6.

- [7] Coue D, Wilson G. A four-quadrant subthreshold mode multiplier for analog neural-network applications. *IEEE Trans Neural Netw* 1996;7(5):1212–9.
- [8] Chang CC, Liu SI. Weak inversion four-quadrant multiplier and two-quadrant divider. *Electron Lett* 1998;34(22):2079–80.
- [9] Gravati M, Valle MG, Ferri G, Guerrini N, Reyes N. A novel current-mode very low power analog CMOS four quadrant multiplier. In: *Proceedings of Solid-State Circuits Conference, ESSCIRC*. 2005. p. 495–8.
- [10] Al-Absi MA, Hussein A, Abuelma'atti MT. A low voltage and low power current-mode analog computational circuit. *Circuits Syst Signal Process* 2013;32(1):321–31.
- [11] Oliaei O, Loumeau P. Four-quadrant class AB CMOS current multiplier. *Electron Lett* 1996;32(25):2327–9.
- [12] Wawryn K. AB class current mode multipliers for programmable neural networks. *Electron Lett* 1996;32(20):1902–4.
- [13] Hyogo A, Fukutomi Y, Sekine K. Low voltage four-quadrant analog multiplier using square-root circuit based on CMOS pair. In: *Proceedings of circuits and systems ISCAS*, vol. 2; 1999. p. 274–7.
- [14] Menekay S, Tarcen RC, Kuntman H. Novel high-precision current-mode multiplier/divider. *Analog Integr Circuits Signal Process* 2009;60(3):237–48.
- [15] Kashitban MM, Khoei A, Hadidi K. A current-mode, first-order Takagi-Sugeno-Kang Fuzzy logic controller, supporting rational-powered membership functions. *IEICE Trans Electron* 2007;E90-C(6):1258–66.
- [16] Hashiesh MH, Mahmoud SA, Soliman AM. New four-quadrant CMOS current-mode and voltage-mode multipliers. *Analog Integr Circuits Signal Process* 2005;45(3):295–307.
- [17] Alikhani A, Ahmadi A. A novel current-mode four-quadrant CMOS analog multiplier/divider. *AEU – Int J Electron Commun* 2012;66(7):581–6.
- [18] Peymanfar A, Khoei A, Hadidi K. Design of a general propose neuro-fuzzy controller by using modified adaptive-network-based fuzzy inference system. *AEU – Int J Electron Commun* 2010;64(5):433–42.
- [19] Minaei S, Yuce E. New squarer circuits and a current-mode full-wave rectifier topology suitable for integration. *Radio Eng* 2010;19(4):657–61.
- [20] Hidayat R, Dehghan K, Moungnoul P, Miyana Y. A GHz simple CMOS squarer circuit. In: *IEEE International Symposium on Communications and Information Technologies, ISCIT*. 2008. p. 539–42.
- [21] Al-Tamimi KM, Al-Absi MA. An ultra-low power high accuracy current-mode CMOS squaring circuit. In: *International Conference of Electrical and Electronics Engineering*. 2012. p. 872–4.
- [22] Wisetphanichkij S, Singkrajom N, Kumngern M, Dehghan K. A low-voltage CMOS current squarer circuit. In: *IEEE International Symposium on Communications and Information Technology, ISCIT*. 2005. p. 271–4.
- [23] Danesh MH, Mahmoudian E, Emami Fard A. A new current-mode squarer circuit for RMS-to-DC converter. *Int J Eng Innovative Technol (IJEIT)* 2013;3(2).
- [24] Sakul C. A new CMOS squaring circuit using voltage/current input. In: *The 23rd International Technical Conference on Circuits/Systems, Computers and Communications*. 2008. p. 525–8.

- [25] Kumngern M, Dehghan K. Versatile dual-mode class-AB four-quadrant analog multiplier. *Int J Signal Process* 2005;2(4).
- [26] De La Cruz-Blas CA, Lopez-Martin AJ, Carlosena A. 1.5 V four-quadrant CMOS current multiplier/divider. *Electron Lett* 2003;39(5):434–6.
- [27] Popa C. Improved accuracy current-mode multiplier circuits with applications in analog signal processing. *IEEE Trans Very Large Scale Integr (VLSI) Syst* 2014;22(2):443–7.
- [28] Ravindran A, Ramarao K, Vidal E, Ismail M. Compact low voltage four quadrant CMOS current multiplier. *Electron Lett* 2001;37(24):1428–9.
- [29] Prommee P, Somdunyanok M, Kumngern M, Dehghan K. Single low-supply current-mode CMOS analog multiplier circuit. In: *IEEE International Symposium on Communications and Information Technologies, ISCIT*. 2006. p. 1101–4.
- [30] Oliveira VJS, Oki N. Low voltage four-quadrant current multiplier: an improved topology for n-well CMOS process. In: *International Conference on Design & Technology of Integrated Systems in Nanoscale Era*. 2007. p. 52–5.



Naser Beyraghi was born in Urmia, Iran, in 1986. He received the B.S. degree in Electrical Engineering from Urmia Azad University, Iran in 2010 and the M.S. degree of electrical engineering in Urmia University, Iran in 2013. His research interests are analog integrated circuit design and fuzzy systems.



Abdollah Khoei was born in Urmia, Iran. He received B.S., M.S., and Ph.D. degrees in electrical engineering from North Dakota State University, USA, in 1982, 1985, and 1989, respectively. His research interests are analog and digital integrated circuit design for fuzzy and neural network applications, fuzzy based industrial electronics and DC–DC converters for portable applications. He is currently with Electrical Engineering Department and Micro-electronics Research Laboratory in Urmia University, Urmia, Iran.